Study of the Effect of the Helical Ripple Transport on the Confinement via Zonal Flows in Helical Plasmas

Shinichiro TODA and Kimitaka ITOH

National Institute for Fusion Science, 322-6 Oroshi-cho, Toki 509-5292, Japan

(Received 7 December 2009 / Accepted 13 March 2010)

The role of the effective helical ripple in the helical plasma confinement is analyzed using the transport code via the effect of zonal flows. One-dimensional coupled transport equations are calculated in the different cases of the effective helical ripple. The reduction of the effective helical ripple ratio lowers the criterion for the excitation of zonal flows in helical plasmas. It is demonstrated that the reduction of the turbulent transport can be obtained in the case of the smaller neoclassical transport when zonal flows are excited.

Keywords: plasma confinement, helical plasma, effective helical ripple, zonal flow, radial electric field

DOI: 10.1585/pfr.5.S2023

1. Introduction

The control of zonal flows is the key issue in fusion research. There has been much progress of the experiments on zonal flow [1]. A number of the calculations have been done and shown the significance of the nonlinear interaction between zonal flows and the turbulence driven by the drift wave (e.g., [2]), suggesting the new framework in the simulations of plasma transport. Based on this paradigm, we have examined the reduction of the turbulent transport due to the excitation of zonal flows by the transport code analysis in the core region of helical plasmas [3]. The electron Internal Transport Barrier (e-ITB) in helical plasmas was shown to be formed by the mechanisms of (i) the bifurcation of the ambipolar electric field and the reduction of the neoclassical energy transport, (ii) the formation of the electric field interface which quenches the turbulence due to the shear of the electric field and (iii) the reduced damping of zonal flows which causes the suppression of the turbulent transport. The transport reduction can be obtained in a wide region for E_r in conjunction with the e-ITB. This shows that the change of the damping of zonal flows can cause the transition in the turbulent transport.

In the collisionless plasmas of the Large Helical Device (LHD) in the region of the small negative electric field, if the ripple transport becomes smaller, the level of the turbulent transport gets lower. We focus on the effect of the helical ripple related with zonal flows on the confinement in the helical plasmas. The reduction of the effective helical ripple causes the smaller damping rate of zonal flows in the helical plasmas even in the branch of the small negative electric field (the ion root), which means the reduction of the turbulent transport. Not only the neoclassical but also turbulent transport is reduced by the inward shift of the magnetic axis in LHD [4, 5]. In the inward shifted configuration of the magnetic axis, the helical ripple transport is found to be much smaller than that in the standard configuration of magnetic axis [6]. In the cases of the different values for the effective helical ripple, the calculation results including the effects of zonal flows will be shown. This study is to investigate the impact of shifting axis positions, because the value of the effective helical ripple changes due to the variation of the experimental magnetic axis positions in LHD. This calculation result will explain the observations on LHD.

2. One-dimensional Model of Transport Equations

The one-dimensional transport model is employed. The cylindrical coordinate is used and r-axis is taken in the radial cylindrical plasma in this article. The region $0 < \rho < 1$ is considered, where $\rho = r/a$ and a is the minor radius. The temporal equations calculated here for the density (n), the temperatures (the electron temperature T_e and the hydrogen ion temperature T_i) and the radial electric field (E_r) in this article are same as those given in [3]. The expression for the radial neoclassical flux associated with helical-ripple trapped particles is given in [7] which covers the collisionless regime (from the ν_j regime to the $1/\nu_\mathrm{j}$ regime), where ν_j is the collision frequency of species j. A theoretical model for the turbulent heat diffusivity χ_T in the presence of zonal flows is adopted [8] . The value for the radial electric field in a nonaxisymmetric system is basically determined by the ambipolar condition [9]. However, the solution of the radial electric field, which satisfies the Maxwell construction [10, 11], can be chosen from the multiple ambipolar E_r when the temporal equation of E_r is used.

author's e-mail: toda@nifs.ac.jp

3. Model of Sources and Boundary Conditions

The source profiles are here set as followed. To establish the plasma, the particle source term S_n is set to be $S_n = S_0 \exp((r-a)/L_0)$. Here the coefficient S_0 is taken as $7 \times 10^{22}\,\mathrm{m^{-3}\,s^{-1}}$ and L_0 is set to be 0.01 m. This profile represents the peaking at the plasma edge of the particle source due to the ionization. Throughout the calculation in this article, the radial profiles of the electron and ion terms of the absorbed powers, P_{he} and P_{hi}, are assumed to be $\exp(-(r/(0.2a)^2)$ for the sake of the analytic insight. The absorbed powers of electrons and ions are set to be 1 MW and 500 kW, respectively.

We choose the boundary condition at the center of the plasma ($\rho = 0$) such that $n' = T_e' = T_i' = E_r = 0$, where the prime denotes the derivative of the physical quantity. At the edge ($\rho = 1$), we employ these boundary conditions, $-n/n' = 0.05$ m, $-T_e/T_e' = -T_i/T_i' = 0.02$ m in this article. For the diffusion equation of the radial electric field, the boundary condition at the edge ($\rho = 1$) is chosen as $\Gamma_e^{na} = \Gamma_i^{na}$, where Γ_e^{na} and Γ_i^{na} represent the nonaxymmetric (neoclassical) part of the particle flux of electrons and the hydrogen ion, respectively. The machine parameters which are similar to those of LHD are set to be $R = 3.6$ m, $a = 0.6$ m, $B = 3$ T, $\ell = 2$ and $m = 10$. In this case, we set the safety factor and the helical ripple coefficient as $q = 1/(0.4 + 1.2\rho^2)$ and $\epsilon_{h0} = 2\sqrt{1 - (2/(mq(0)) - 1)}\, I_2(mr/R)$, respectively [12]. Here, $q(0)$ is the value of the safety factor at $\rho = 0$ and I_2 is the second-order modified Bessel function.

4. Model of Turbulent Transport Coefficients

In the absence of the zonal flow, the model for the anomalous heat diffusivity χ_a is adapted as a candidate, which is based on the theory of the self-sustained turbulence due to the ballooning mode and the interchange mode, both driven by the current diffusivity [13, 14]. The reduction of the anomalous transport due to the inhomogeneous radial electric field was reported in the toroidal helical system. The anomalous heat transport coefficient is given as $\chi_a = \chi_0/(1 + G\omega_{E1}^2)$ ($\chi_0 = F(s,\alpha)\alpha^{\frac{3}{2}} c^2 \nu_A/(\omega_{pe}^2 qR)$), where ω_{pe} is the electron plasma frequency. The factor $F(s,\alpha)$ is the function of the magnetic shear s and the normalized pressure gradient α. For the ballooning mode turbulence (in the system with a magnetic well) [13], we employ the anomalous thermal conductivity $\chi_{a,BM}$. In the case of the interchange mode turbulence for the system of the magnetic hill [14], we adopt the anomalous thermal conductivity $\chi_{a,IM}$. The details on the coefficients $F(s,\alpha)$, G and the factor ω_{E1}, which stands for the poloidal $E \times B$ rotation frequency, are given in [13, 14] in the ballooning and interchange mode turbulence, respectively. The greater one of these two diffusivities is adopted as $\chi_a = max(\chi_{a,BM}, \chi_{a,IM})$.

In this article, we use the same procedure to derive the value of the turbulent heat diffusivity in the presence of zonal flows with that in [3]. Zonal flows (at nearly zero frequency) are generated by the fluctuations and strongly influence the turbulent transport. The damping of zonal flows is caused by the collisional process [15] and by the self-nonlinearity of zonal flows [2]. Whether zonal flows are excited or not is judged by comparing with the quantity [8, 16], $\chi_{damp} \simeq k_\perp^2 q_r^{-2} k_\theta^{-2} \nu_{damp}$, where q_r is the wave number of zonal flows, k_θ is the poloidal wave number and $k_\perp$ are the perpendicular wave number of the microscopic fluctuations, respectively. When the turbulence is weak and χ_a is smaller than χ_{damp}, zonal flows are not excited and one has $\chi_T = \chi_a$. If the condition $\chi_{damp} < \chi_a$ satisfies, the turbulent diffusivity χ_T is reduced as $\chi_T = \sqrt{\chi_a \chi_{damp}}$ [8]. A fitting interpolation formula is employed as $\chi_T = \sqrt{\chi_a}\min(\sqrt{\chi_a}, \sqrt{\chi_{damp}})$ to include the effect of zonal flows in the transport codes. The damping rate of the $\boldsymbol{E} \times \boldsymbol{B}$ (poloidal) flow ν_{pf} is defined as $-(\partial(\delta U_p)/\partial t)/\delta U_p$, where U_p is the speed of the poloidal flow and δ shows the perturbed component. If we assume the relation $U_p = -E_r/B$, the damping rate is shown as $-(\partial(\delta E_r)/\partial t)/\delta E_r$. Therefore, we obtain the damping rate $\nu_{pf} = \partial J_r^{na}/\partial E_r/\epsilon_\perp$ from the differential equation in terms of E_r [16]. The neoclassical part of the radial current $J_r^{na}(= e(\Gamma_i^{na} - \Gamma_e^{na}))$ in helical plasmas has a nonlinear dependence on E_r. We obtain the damping rate ν_{damp} of zonal flows as $\nu_{damp} = \min(\nu_{thi}/qR, \nu_{ii}/\epsilon) + \nu_{pf}$, where ν_{thi} is the thermal velocity of ions and ν_{ii} is the collision frequency of ions. The first term takes the smaller value between the term $\nu_{thi}/(qR)$ and the term ν_{ii}/ϵ, which represents the collisional damping rate in the plateau and banana regimes without the E_r effect, respectively. The second term comes from the dependence of the neoclassical current on the radial electric field. Owing to the dependence of ν_{damp} on E_r, the value of ν_{damp} is large in the weak positive and negative solution of E_r, while it is small in the strong positive and negative E_r solution, in the typical parameter region of experimental results in helical plasmas. The turbulent transport coefficient becomes smaller when the strong positive radial electric field is formed in the e-ITB. [3, 16]

For simplicity, the value for the turbulent diffusivities of the particle is set as $D_T = 10\,\mathrm{m^2/s}$. The essence of the results shown later does not change due to the value of D_T. The value of D_T is set to be constant spatially and temporally. We also set $D_{ET} = \chi_T$ for the diffusion coefficient of the radial electric field in order to examine the variation of the typical length for the electric field shear at the transition point.

5. Results of the Analysis

The effect of the helical ripple transport on the confinement via zonal flows in helical plasmas is studied by use of the transport code analysis. We show the calculation results for two cases of the effective helical ripple:

$\epsilon_h = \epsilon_{h0}$ and $\epsilon_h = 0.1\epsilon_{h0}$. In the cases of $\epsilon_h = \epsilon_{h0}$ and $\epsilon_h = 0.1\epsilon_{h0}$, the calculations in the standard configuration and the inward-shifted configuration in LHD experiments are demonstrated, respectively. The helical ripple transport in the inward shifted configuration is much smaller than that in the standard configuration in the experimental results in LHD. One-dimensional transport model analysis for the LHD-like plasmas has been done. The profiles of n, T_e, T_i and E_r are solved as an initial value problem adopting the turbulent transport diffusivities with the effect of zonal flows. An example is taken from the plasma which is sustained by the electron cyclotron resonance (ECR) heating. In order to set the line-averaged temperature of electrons to be around $\bar{T}_e = 2.0\,\mathrm{keV}$ and the line-averaged density to be around $\bar{n} = 1.6 \times 10^{19}\,\mathrm{m}^{-3}$, for the choice of the above mentioned turbulent transport coefficients. The line-averaged ion temperature $\bar{T}_i$ is chosen to be about $\bar{T}_i = 1.2\,\mathrm{keV}$. The central ion heating is used in the present calculations, because the importance of the ratio T_e/T_i was already remarked to obtain the E_r transition between the ambipolar multiple E_r [17]. When we evaluate χ_{damp}, we employ an estimate $k_\perp^2 q_r^{-2} k_\theta^{-2} \rho_i^{-2} \sim 50$ [8].

The stationary profiles of the radial electric field (a), the density (b), the electron temperature (c) and the ion temperature (d) are demonstrated in Fig. 1 as a calculation result when zonal flows are excited in the two cases of the effective helical ripple. The solid line shows the case: (1) $\epsilon_h = \epsilon_{h0}$, which corresponds to the experimental situation of the standard configuration, $R_{ax} = 3.75\,\mathrm{m}$ in LHD. The dashed line represents the case of the smaller helical ripple: (2) $\epsilon_h = 0.1\epsilon_{h0}$, which corresponds to the experimental situation of the inward shifted configuration, $R_{ax} = 3.6\,\mathrm{m}$. In Fig. 1 (a), the radial transition from the positive radial electric field to the negative one is shown. The parameter ρ_T represents the location of this radial transition of E_r. In both cases of the effective helical ripple, the steep gradient of E_r can be obtained. Therefore, the improvement near the transition point is obtained in the narrow region due to the steep E_r gradient. It is found that the radial electric field is strongly positive in the region $\rho < \rho_T$, $|E_r| > 25\,\mathrm{kV/m}$. On the other hand, the radial electric field is slightly negative in the region $\rho > \rho_T$, $|E_r| < 10\,\mathrm{kV/m}$. In the case of the smaller helical ripple: $\epsilon = 0.1\epsilon_{h0}$, the value of the radial electric field gets larger than the case: $\epsilon = \epsilon_{h0}$ in the region $\rho < \rho_T$. The stationary profiles of the density are shown in the two cases of the effective helical ripple in Fig. 1 (b). The profiles of the density do not differ significantly due to lowering the value of the effective helical ripple, because the turbulent particle diffusivity is set constant as $D_T = 10\,\mathrm{m}^2/\mathrm{s}$ in the calculations here. We also obtain the stationary profiles of the electron temperature (c) and the ion temperature (d) in two cases of the effective helical ripple in Fig. 1. The clear change of the gradient for the electron and ion temperatures at the transition point ρ_T can be obtained in both cases of the effective helical ripple, that shows the characteristic of the transport barrier.

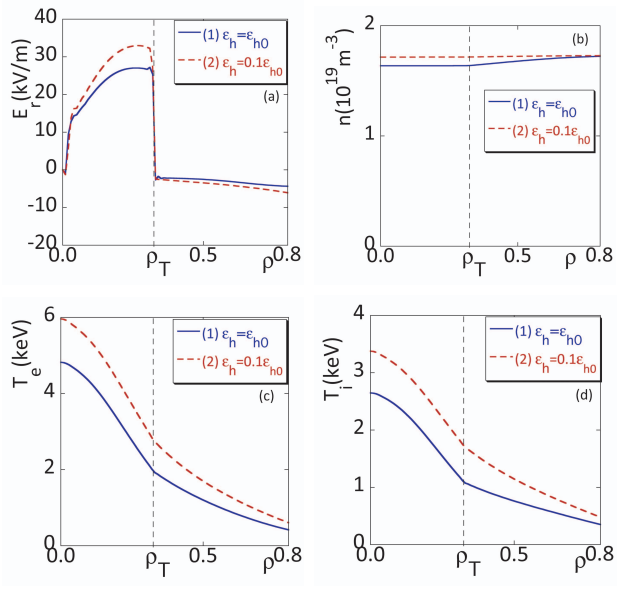

Fig. 1 Radial profiles of (a) the electric field, (b) the density, (c) the electron temperature and (d) the ion temperature for the two cases of the effective helical ripple: $\epsilon_h = \epsilon_{h0}$ with the solid line and the smaller helical ripple: $\epsilon_h = 0.1\epsilon_{h0}$ with the dashed line.

Next, the effect of the helical ripple via zonal flows is examined in the calculation results. The radial profiles of the criterion for the excitation of zonal flows, χ_{damp} (the solid line), the turbulent heat diffusivity without the effect of zonal flows, χ_a (the dashed line) and the turbulent heat diffusivity with the effect of zonal flows, χ_T (the dotted line), are shown in Fig. 2. The radial profiles of the heat diffusivity are shown in the case: $\epsilon_h = \epsilon_{h0}$ in Fig. 2 (a). On the other hand, in Fig. 2 (b), the radial profiles of the heat diffusivity are shown in the case: $\epsilon_h = 0.1\epsilon_{h0}$ in Fig. 2 (b). If the relation $\chi_{\mathrm{damp}} < \chi_a$ is satisfied, zonal flows are excited. In both cases in Fig. 2, the reduction is obtained from the heat diffusivity without the effect of zonal flows χ_a to the turbulent heat diffusivity with the effect of zonal flows χ_T in the entire core region $\rho < \rho_T$. The damping rate of zonal flows is small if the value of E_r is large such as $E_r \simeq 30\,\mathrm{kV/m}$ in the region $\rho < \rho_T$ in Fig. 1 (a), because the neoclassical radial current has a weak dependence on the radial electric field in the region where the absolute value of E_r becomes large. These results are same as those in [3]. In the outer region $\rho > \rho_T$ of Fig. 2 (a), the criterion for the excitation of zonal flows, χ_{damp} is larger than the turbulent heat diffusivity without the effect of zonal flows, χ_a. Therefore, the reduction from χ_a to χ_T due to zonal flows does not occur in the outer region $\rho > \rho_T$ in the case: $\epsilon_h = \epsilon_{h0}$. On the other hand, in Fig. 2 (b), the criterion for the excitation of zonal flows, χ_{damp} gets smaller than χ_a in the region $\rho > \rho_T$, because the smaller effective helical ripple ratio lowers the criterion for the excitation of zonal flows χ_{damp}. This case: $\epsilon_h = 0.1\epsilon_{h0}$ corresponds to the experimental condition of the inward shifted configuration

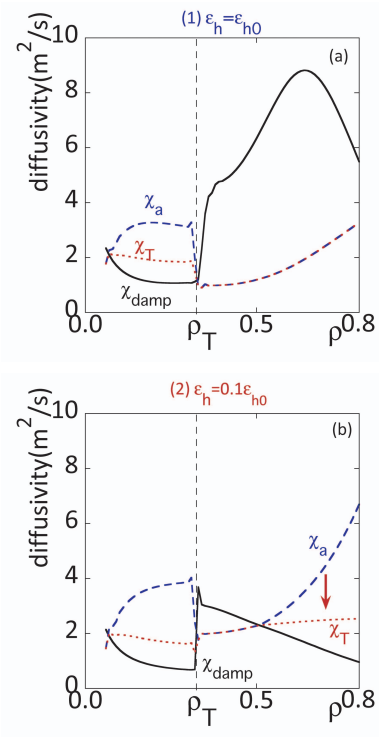

Fig. 2 Radial profiles of the heat diffusivitiy in the case of (a) $\epsilon_h = \epsilon_{h0}$ and (b) $\epsilon_h = 0.1\epsilon_{h0}$. The solid line, the dashed line and the dotted line show the radial profiles of χ_{damp} of the criterion for the excitation of zonal flows, the turbulent diffusivity in the absence of zonal flow and the turbulent diffusivity with the effect of zonal flows, respectively.

in LHD. The damping rate of zonal flows is mainly determined by the damping rate of the $\boldsymbol{E} \times \boldsymbol{B}$ (poloidal) flow rather than the collisional damping in the parameter region examined here. Since the effective helical ripple gets smaller, the damping rate of zonal flows also gets smaller, even if the absolute value of E_r is less than 10 kV/m in the region $\rho > \rho_T$ in Fig. 1 (a). Therefore, the reduction from χ_a to χ_T due to zonal flows is obtained in Fig. 2 (b) even in the outer region $\rho > \rho_T$, where the radial electric field takes the small (negative) value. In the core region $\rho > \rho_T$, the value of χ_T in the case: $\epsilon_h = 0.1\epsilon_{h0}$ is smaller than that in the case: $\epsilon_h = \epsilon_{h0}$, because of the larger positive value of E_r in the case: $\epsilon_h = 0.1\epsilon_{h0}$. However, the value of χ_T in the case: $\epsilon_h = 0.1\epsilon_{h0}$ is larger than that in the case: $\epsilon_h = \epsilon_{h0}$ in the region $\rho_T < \rho < 0.7$. This is because the value of χ_a in the case: $\epsilon_h = 0.1\epsilon_{h0}$ is larger than that in the case: $\epsilon_h = \epsilon_{h0}$, where the values of n, T_e, T_i, $|T_e'|$ and $|T_i'|$ become larger in the case: $\epsilon_h = 0.1\epsilon_{h0}$ comparing with the case: $\epsilon_h = \epsilon_{h0}$. This result depends on the choice of the model for the anomalous heat diffusivity, χ_a. The value of χ_T in the case: $\epsilon_h = 0.1\epsilon_{h0}$ is smaller than that in the case: $\epsilon_h = \epsilon_{h0}$ in the region $\rho > 0.7$, because the reduction from χ_a to χ_T due to zonal flows is obtained in Fig. 2 (b) in the outer region $\rho > \rho_T$. The significant reduction of the total heat diffusivities, (the sum of the neoclassical and turbulent heat diffusivities), is found specially in the region $\rho > \rho_T$ in

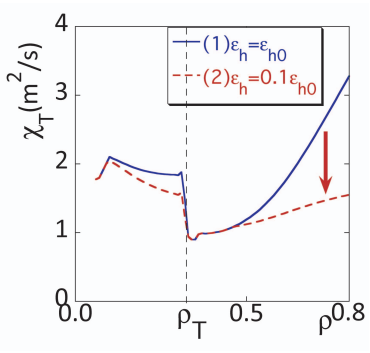

Fig. 3 Radial profile of the turbulent diffusivity in the presence of zonal flows from the same profiles of the density, the temperatures and the electric field. The solid line and the dashed line show in the cases of $\epsilon_h = \epsilon_{h0}$ and $\epsilon_h = 0.1\epsilon_{h0}$.

the case of $\epsilon_h = 0.1\epsilon_{h0}$ comparing with the case of $\epsilon_h = \epsilon_{h0}$, due to the reduction of the neoclassical transport. Finally, the analysis is performed to compare the heat turbulent diffusivities when zonal flows are excited in two cases of the effective helical ripple for the same plasma profiles (n, T_e, T_i and E_r) . The plasma profiles in the case: $\epsilon_h = \epsilon_{h0}$ in Fig. 1 are used. The radial profiles of χ_T are shown in the case: $\epsilon_h = \epsilon_{h0}$ with the solid line and in the case of the smaller helical ripple: $\epsilon_h = 0.1\epsilon_{h0}$ with the dashed line in Fig. 3. Even in the outer region $\rho > \rho_T$, the reduction of χ_T in the case of the smaller helical ripple can be obtained, comparing with the case: $\epsilon_h = \epsilon_{h0}$, because the smaller effective helical ripple lowers the criterion for the excitation of the zonal flows.

6. Summary

In summary, one-dimensional transport analysis in helical plasmas is performed in the different cases of the effective helical ripple to examine the effect of the ripple transport on confinement via zonal flows. Even in the outer region where the small negative E_r is shown, the reduction of the turbulent transport can be obtained in the case of smaller helical ripple when zonal flows are excited. This is because the reduction of the effective helical ripple ratio lowers the criterion for the excitation of zonal flows, especially the damping rate of $\boldsymbol{E}\times\boldsymbol{B}$ (poloidal) flow. This model with the effect of zonal flows used here may be a candidate to explain the transport reduction in the outer region (of the small negative electric field) observed in the case of the inward shifted configuration ($R_{ax} = 3.6$ m) in LHD. In this article, the damping of zonal flows was mainly addressed, because the drive of zonal flows is not shown in the parameter region examined here. If the effective helical ripple changes, the drive of zonal flows may be seen. The study of this article is not limited to toroidal helical plasmas, should be extended to the tokamak plasmas. In the extension to the tokamak plasmas, the main and interesting subject is what physical mechanisms determine the structure of the radial electric field in tokamaks. This work

is left for the future study.

This work is performed with the support and the auspices of the NIFS Collaborative Research Program, Nos. NIFS08KLDD014 and NIFS08KNXN122.

[1] A. Fujisawa, Nucl. Fusion **49**, 013001 (2009).
[2] P. H. Diamond *et al.*, Plasma Phys. Control. Fusion **47**, R35 (2005).
[3] S. Toda *et al.*, Nucl. Fusion **47**, 914 (2007).
[4] H. Yamada *et al.*, Plasma Phys. Control. Fusion **43**, A55 (2001).
[5] K. Ida *et al.*, Phys. Rev. Lett. **86**, 5297 (2001).
[6] K. Ida *et al.*, Nucl. Fusion **45**, 391 (2005).
[7] K. C. Shaing, Phys. Fluids **427**, 1567 (1984).
[8] K. Itoh *et al.*, Phys. Plasmas **12**, 062303 (2005).
[9] K. Ida, Plasma Phys. Control. Fusion **40**, 1429 (1998).
[10] H. Haken, *Synergetics* (Spring-Verlag, 1983) Sec. 9.3.
[11] F. Schlögl, Z. Physik **253**, 147 (1972).
[12] H. Sanuki *et al.*, J. Phys. Soc. Japan **69**, 445 (2000).
[13] K. Itoh *et al.*, Plasma Phys. Control. Fusion **36**, 279 (1994).
[14] K. Itoh *et al.*, Plasma Phys. Control. Fusion **36**, 123 (1994).
[15] M. Taguchi, Plasma Phys. Control. Fusion **33**, 859 (1991).
[16] K. Itoh *et al.*, Phys. Plasmas **14**, 020702 (2007).
[17] S. Toda and K. Itoh, Plasma Phys. Control. Fusion **44**, A501 (2002).